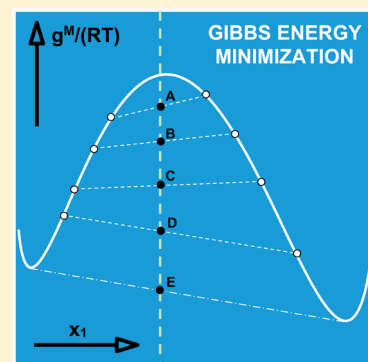


Teaching the Concept of Gibbs Energy Minimization through Its Application to Phase-Equilibrium Calculation

Romain Privat,* Jean-Noël Jaubert,* Etienne Berger, Lucie Coniglio, Cécile Lemaitre, Dimitrios Meimaroglou, and Valérie Warth

Laboratoire Réactions et Génie des Procédés (UMR CNRS 7274), Ecole Nationale Supérieure des Industries Chimiques, Université de Lorraine, 1 rue Grandville, 54000 Nancy, France

ABSTRACT: Robust and fast methods for chemical or multiphase equilibrium calculation are routinely needed by chemical-process engineers working on sizing or simulation aspects. Yet, while industrial applications essentially require calculation tools capable of discriminating between stable and nonstable states and converging to nontrivial solutions, students are often introduced to the simplest and less efficient equilibrium-calculation methods. In this article, the Gibbs energy minimization technique is presented as a robust alternative way to perform phase-equilibrium calculations and is applied to the determination of 2-fluid phase equilibria in low-pressure binary systems. It is carefully explained how the combination of this technique with an efficient quasi-global minimization method makes it possible to derive a robust PT-flash algorithm. In the frame of project-based learning devoted to develop a tool for building complex phase diagrams, this approach was successfully tested with a group of 100 students.



KEYWORDS: Chemical Engineering, Graduate Education/Research, Thermodynamics, Phases/Phase Transitions/Diagrams, Equilibrium, Computer-Based Learning

INTRODUCTION

Phase-equilibrium calculations are routinely used in chemical engineering applications such as single-stage and multistage processes (including flash drum, distillation, absorption, extraction, etc.) which bring two fluid phases into contact (e.g., two liquid phases or a liquid phase and a vapor phase). For this reason, the teaching of phase-equilibrium calculations and dedicated algorithms takes a preeminent place in most modern chemical engineering courses. Nevertheless, whereas new and novel approaches to perform phase-equilibrium calculations are continuously emerging, undergraduate students are traditionally introduced to the oldest and most basic vapor–liquid equilibrium (VLE) solving method (i.e., the Rachford–Rice method to perform PT-flash calculations).

The present article specifically addresses the PT-flash problem which aims at determining whether a multicomponent mixture of known overall composition z , at a specified temperature T and pressure P , is made up of one or two phases; in the latter case, the composition and the proportions of the two equilibrium phases must be determined.

The implementation of such methods requires coupling material-balance equations with phase-equilibrium conditions. Mainly two different ways can be used to do so:

1. The first and more traditional approach lies in writing
 - the material-balance equations,

$$z_i = \tau_\alpha x_i^\alpha + \tau_\beta x_i^\beta \quad \text{with} \quad \tau_\beta = 1 - \tau_\alpha \quad (1)$$

where z_i is the overall mole fraction of component i , x_i^k is the mole fraction of i in phase $k \in \{\alpha, \beta\}$, and τ_k is the molar proportion of phase k ;

- the phase-equilibrium condition expressed through the equality of the chemical potentials of each component in the two equilibrium phases,

$$\mu_i^\alpha(T, P, \mathbf{x}^\alpha) = \mu_i^\beta(T, P, \mathbf{x}^\beta) \quad \forall i \in \{1, \dots, p\} \quad (2)$$

where p denotes the number of components in the mixture and \mathbf{x}^k is the vector of the component mole fractions in phase k .

Addressing the specific case of binary systems ($p = 2$) in 2-phase equilibrium at fixed T and P , the equilibrium mole-fraction vectors $\mathbf{x}^\alpha = (x_1^\alpha; 1 - x_1^\alpha)$ and $\mathbf{x}^\beta = (x_1^\beta; 1 - x_1^\beta)$ are calculated by solving a system of 2 equations (i.e., eq 2 written for $i = 1$ and $i = 2$). From a graphical point of view, x_1^α and x_1^β are the abscissa of the 2 tangent points located on a double tangent (i.e., a tangent common to 2 different points of the same curve) to the curve Gibbs energy change on mixing g^M of the single-phase mixture versus overall mole fraction of component 1. As an example, Figure 1a shows the double-tangent construction for a binary system in liquid–liquid equilibrium. Algorithms

Received: March 28, 2016

Revised: June 16, 2016

Published: July 5, 2016

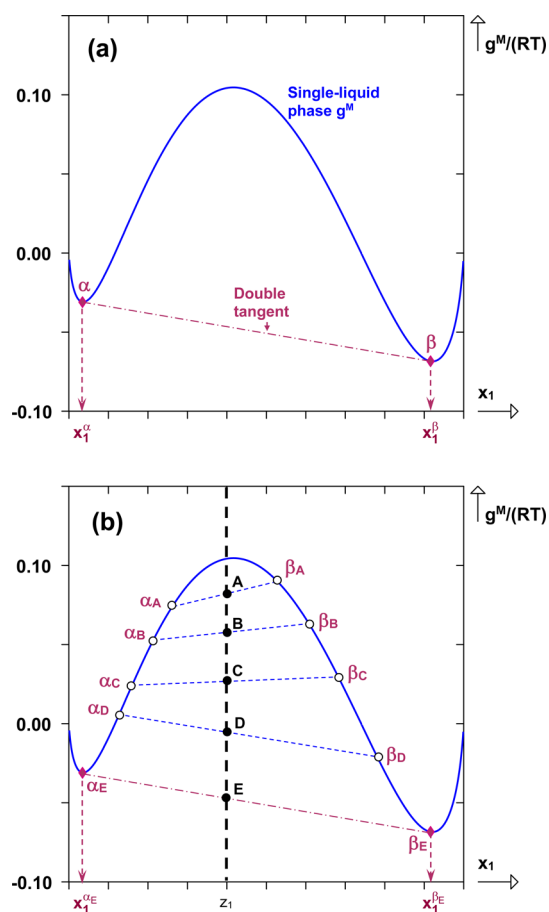


Figure 1. Illustration of 2 techniques for determining mole fractions of 2 liquid phases in equilibrium in a binary system, at fixed temperature and pressure. Blue curve: single liquid phase Gibbs energy change on mixing. (a) Determination of phase-equilibrium compositions using the double-tangent construction. (b) Determination of phase-equilibrium compositions for an overall mole fraction z_1 using a Gibbs energy minimization procedure.

implementing this approach (or similar ones) can be easily found in the open literature.^{1–3}

- The second approach lies in searching the phase-equilibrium compositions at fixed T and P as the ones minimizing the molar total Gibbs energy change on mixing of the two-phase mixture of overall composition z . To do so, initial values are affected to phase compositions x^α and x^β which are then changed in order to make the molar total Gibbs energy change on mixing of the mixture decrease up to its smallest possible value. As an illustration, a series of schematic optimization procedure steps are represented in Figure 1b for the same binary system as previously. The initial guessed values of phase compositions are $x_1^{\alpha_A}$ and $x_1^{\beta_A}$. The corresponding molar total Gibbs energy change on mixing value at overall composition z_1 is g_A^M (see point A). By modifying the phase compositions x_1^α and x_1^β (using an appropriate minimization algorithm), the Gibbs energy change on mixing takes successively the values g_B^M , g_C^M , g_D^M (see points B, C, D, respectively) to reach its final minimal value g_E^M (see point E) associated with phase-equilibrium compositions $x_1^{\alpha_E}$ and $x_1^{\beta_E}$.

The flash-equilibrium problem at fixed T and P (see the definition of a PT-flash problem above) can thus be formulated either as a nonlinear equation solving problem or as a

minimization problem. Note that both approaches are actually not rigorously equivalent since the chemical potential equality (see eq 2) is a necessary but not a sufficient condition to ensure that a stable state is reached (stable means here that the Gibbs energy change on mixing of the equilibrium mixture is the smallest possible one). In other words, the solving of eq 2 may result in nonstable state solutions whereas a successful global Gibbs minimization technique ensures that a stable state is found.

In the open literature dedicated to education aspects, Gibbs energy minimization techniques are essentially illustrated through examples dealing with chemical-reaction equilibrium search.^{4,5} This article is aimed at sharing a pedagogical experience that was implemented in the ENSIC School (chemical engineering department of the University of Lorraine, in France). In the framework of a project, master students were invited to compute complex fluid-phase diagrams. To do so, they realized first a PT-flash algorithm based on Gibbs energy minimization (note that a PT-flash algorithm is aimed at solving a PT-flash problem, as defined above). In a second step, the algorithm was used to generate complete isobaric fluid phase-equilibrium diagrams related to the binary systems *tert*-butanol (1) + water (2) and butan-2-one (1) + water (2). In order to avoid fastidious calculations (and in particular, to avoid solving equations of state), the γ - ϕ approach was used: the liquid phase was described by the NRTL (nonrandom two-liquid) activity-coefficient model whereas the gas phase was assumed to behave as a perfect gas. Regarding minimization aspects, a recent model based on an evolutionary bioinspired algorithm was considered to ensure—as far as possible—global optimization (i.e., to find global minimum over all input values, as opposed to finding local minima).

■ EXPRESSION OF THE FLASH TP PROBLEM FOR BINARY SYSTEMS AS A CONSTRAINED MINIMIZATION PROBLEM

Evolution Criterion at Fixed Temperature and Pressure

According to the second law of thermodynamics, the evolution criterion for a spontaneous arbitrary transformation is

$$\delta S_C \geq 0 \quad (3)$$

with δS_C , the elementary entropy produced during the transformation. For a transformation undergone by a closed system at fixed temperature T and pressure P in mechanical and thermal equilibrium with its surroundings ($T = T_{\text{surroundings}}$ and $P = P_{\text{surroundings}}$), the evolution criterion can be simply expressed in terms of molar Gibbs energy:

$$dg \leq 0 \quad (\text{at fixed } T \text{ and } P) \quad (4)$$

Equivalently, this criterion can be written in terms of molar Gibbs energy change on mixing:

$$dg^M \leq 0 \quad (\text{at fixed } T \text{ and } P) \quad (5)$$

This criterion states that a system at fixed T and P can evolve to a new state if, and only if, the entropy production is positive, i.e., the transformation leads to an overall decrease of its total molar Gibbs energy on mixing.

Application of the Evolution Criterion to the Comparison between 1-Phase System Stabilities

The search for a stable state among different possible single-phase states is an important application of this isothermal isobaric evolution criterion: if, at a specified T and P , two 1-phase

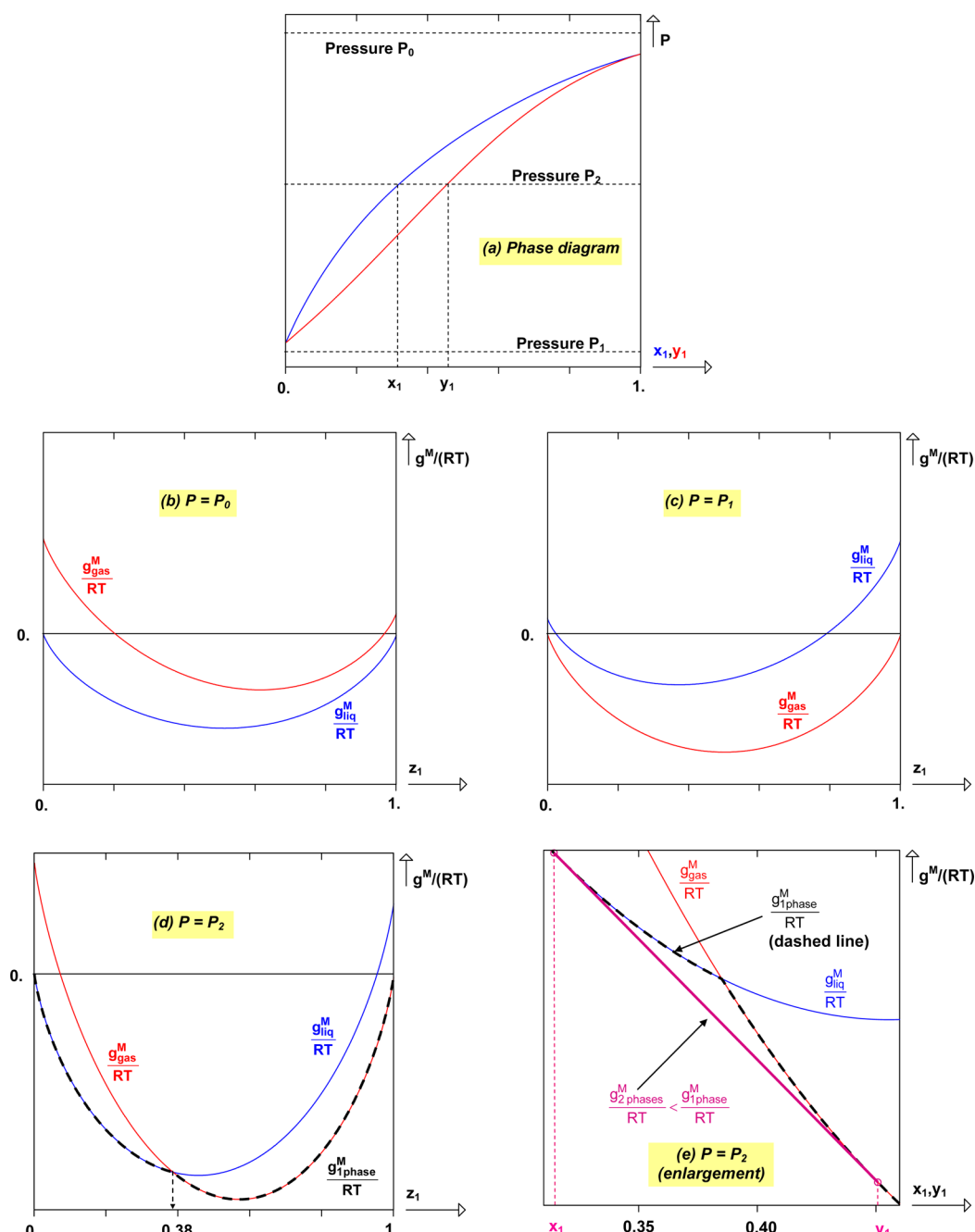


Figure 2. Illustration of the evolution criterion at fixed $T = T_0$ and P . (a) Isothermal vapor–liquid equilibrium phase diagram of a given binary system at $T = T_0$. (b–e) Isothermal and isobaric projections of the reduced total molar Gibbs energy change on mixing $g^M/(RT)$ versus mole fraction of component 1 at $T = T_0$ and P_0 , P_1 , and P_2 (these pressures are defined in panel a).

physical states (denoted α and β) are possible for a given binary mixture of known composition $\mathbf{z} = (z_1; z_2 = 1 - z_1)$, the stable state is the one associated with the lowest g^M value:

$$g_{1\text{phase}}^M(T, P, \mathbf{z}) = \min\{g_{\alpha}^M(T, P, \mathbf{z}); g_{\beta}^M(T, P, \mathbf{z})\} \quad (6)$$

For illustrating this concept, some isobaric and isothermal projections of $g^M/(RT)$ (reduced total molar Gibbs energy change on mixing) versus z_1 (mole fraction of component 1) for a given binary system are represented in Figure 2b–e. The pressures at which these projections are plotted are indicated on the isothermal phase-equilibrium diagram of the binary system at T_0 , see Figure 2a (note that x_1 and y_1 denote the mole fraction of component 1 in the liquid and gas phases, respectively).

At T_0 and P_0 , $g^M/(RT)$ was calculated for the two possible physical states of the single-phase binary system: single liquid and single gas. According to Figure 2b, the Gibbs energy change on mixing of the liquid system g_{liq}^M is lower than the one of the gas system g_{gas}^M for any value of z_1 ; following the evolution criterion, the binary system is thus in a single liquid state under these conditions, as confirmed by the phase diagram and, consequently, $\forall z_1 \in [0; 1]$, $g_{1\text{phase}}^M(T, P, \mathbf{z}) = g_{liq}^M(T, P, \mathbf{z})$.

At T_0 and P_1 , for any value of z_1 , one has $g_{gas}^M < g_{liq}^M$ as shown in Figure 2c. Consequently, $g_{1\text{phase}}^M(T, P, \mathbf{z}) = g_{gas}^M(T, P, \mathbf{z})$ and only the single gas phase is stable at T_0 and P_1 .

According to Figure 2d, for the binary system at the intermediate pressure P_2 , it is observed that

$$\left\{ \begin{array}{l} \text{for } z_1 < 0.38: \quad g_{\text{liq}}^{\text{M}} < g_{\text{gas}}^{\text{M}} \\ \quad \Leftrightarrow g_{1\text{phase}}^{\text{M}}(T, P, \mathbf{z}) = g_{\text{liq}}^{\text{M}}(T, P, \mathbf{z}) \\ \text{for } z_1 > 0.38: \quad g_{\text{gas}}^{\text{M}} < g_{\text{liq}}^{\text{M}} \\ \quad \Leftrightarrow g_{1\text{phase}}^{\text{M}}(T, P, \mathbf{z}) = g_{\text{gas}}^{\text{M}}(T, P, \mathbf{z}) \\ \text{for } z_1 = 0.38: \quad g_{1\text{phase}}^{\text{M}}(T, P, \mathbf{z}) = g_{\text{gas}}^{\text{M}}(T, P, \mathbf{z}) \\ \quad \quad \quad = g_{\text{liq}}^{\text{M}}(T, P, \mathbf{z}) \end{array} \right.$$

Note that the $g_{1\text{phase}}^{\text{M}}$ vs z_1 curve is represented with a dashed line in Figure 2d. If the analysis is limited to the sole comparison of single-phase stabilities, it can be concluded that the single-liquid phase is stable for any $z_1 < 0.38$ whereas the single-gas phase is stable for $z_1 > 0.38$. At $z_1 = 0.38$, it is observed that the single-liquid phase and the single-gas phase are simultaneously stable.

These conclusions could appear surprising since the phase diagram (see Figure 2a) clearly shows that the stable state is actually the vapor–liquid equilibrium on the composition range $[x_1; y_1]$. However, we need here to point out that our previous analysis only focuses on a comparison between single-phase state stabilities. To reach the conclusion that the vapor–liquid equilibrium state is more stable than 1-phase states for any $z_1 \in [x_1; y_1]$, it would be necessary to compare 1-phase and 2-phase state stabilities, which is the purpose of the next section.

Application of the Evolution Criterion to the Comparison of 1-Phase and 2-Phase Mixture Stabilities at Fixed Temperature, Pressure, and Overall Composition

The isothermal isobaric evolution criterion can also be used to determine whether a binary mixture at (T, P, \mathbf{z}) is made up of one phase or two equilibrium phases: if the total molar Gibbs energy change on mixing of the 2-phase system ($g_{2\text{phases}}^{\text{M}}$) is lower than the total molar Gibbs energy change on mixing of the single-phase system ($g_{1\text{phase}}^{\text{M}}$), then the system is in a 2-phase state. Conversely, the system is made up of one single phase if $g_{1\text{phase}}^{\text{M}}$ is lower than $g_{2\text{phases}}^{\text{M}}$.

General Expression of Molar Gibbs Energy Change on Mixing of 2-Phase System. The reduced total molar Gibbs energy change on mixing of a binary system in 2-phase equilibrium (the equilibrium phases are denoted α and β) at a specified temperature T , pressure P , and overall composition $\mathbf{z} = (z_1; z_2 = 1 - z_1)$ is given by eq 7:

$$\frac{g_{2\text{phases}}^{\text{M}}}{RT} = \tau_{\alpha} \frac{g_{\alpha}^{\text{M}}}{RT} + \tau_{\beta} \frac{g_{\beta}^{\text{M}}}{RT} \quad (7)$$

where $g_{\alpha}^{\text{M}} = g_{1\text{phase}}^{\text{M}}(T, P, \mathbf{x}^{\alpha})$ and $g_{\beta}^{\text{M}} = g_{1\text{phase}}^{\text{M}}(T, P, \mathbf{x}^{\beta})$ are the total molar Gibbs energy change on mixing related to the single phases α and β , respectively. According to the lever rule, the molar proportions of phases α and β can be expressed with respect to z , \mathbf{x}^{α} , and \mathbf{x}^{β} :

$$\tau_{\beta} = \frac{z_1 - x_1^{\alpha}}{x_1^{\beta} - x_1^{\alpha}} \quad \text{and} \quad \tau_{\alpha} = 1 - \tau_{\beta} \quad (8)$$

The final expression of $g_{2\text{phases}}^{\text{M}}$ is obtained by combination of eqs 7 and 8:

$$\frac{g_{2\text{phases}}^{\text{M}}(T, P, \mathbf{z}, \mathbf{x}^{\alpha}, \mathbf{x}^{\beta})}{RT} = \frac{x_1^{\beta} - z_1}{x_1^{\beta} - x_1^{\alpha}} \frac{g_{1\text{phase}}^{\text{M}}(T, P, \mathbf{x}^{\alpha})}{RT} + \frac{z_1 - x_1^{\alpha}}{x_1^{\beta} - x_1^{\alpha}} \frac{g_{1\text{phase}}^{\text{M}}(T, P, \mathbf{x}^{\beta})}{RT} \quad (9)$$

Graphical consequence of eq 9: for a binary system in 2-phase equilibrium at T and P , the equilibrium compositions \mathbf{x}^{α} and \mathbf{x}^{β} are fixed (according to the Gibbs phase rule) and the curve $\frac{g_{2\text{phases}}^{\text{M}}(T, P, \mathbf{z}, \mathbf{x}^{\alpha}, \mathbf{x}^{\beta})}{RT}$ versus z_1 is actually a straight line, defined for any $z_1 \in [x_1^{\alpha}; x_1^{\beta}]$, which is tangent in two points to the curve $\frac{g_{1\text{phase}}^{\text{M}}(T, P, \mathbf{z})}{RT}$ versus z_1 that are $(x_1^{\alpha}; g_{1\text{phase}}^{\text{M}}(T, P, \mathbf{x}^{\alpha}))$ and $(x_1^{\beta}; g_{1\text{phase}}^{\text{M}}(T, P, \mathbf{x}^{\beta}))$. Such a straight line is named double tangent.

Use of a Minimization Procedure To Find out Stable 2-Phase States. Following the evolution criterion, a binary system at (T, P, \mathbf{z}) is in a stable two-phase equilibrium if, and only if, it is possible to find x_1^{α} and x_1^{β} values such that

$$g_{2\text{phases}}^{\text{M}}(T, P, \mathbf{z}, \mathbf{x}^{\alpha}, \mathbf{x}^{\beta}) < g_{1\text{phase}}^{\text{M}}(T, P, \mathbf{z}) \quad (10)$$

In such a case, the single-phase binary system is declared nonstable. The stable 2-phase state is found for x_1^{α} and x_1^{β} values leading to the smallest possible value of $g_{2\text{phases}}^{\text{M}}$.

Mathematically speaking, a stable 2-phase equilibrium of a given binary mixture at fixed T, P , and \mathbf{z} can thus be seen as the solution of the following minimization problem:

$$\min_{\substack{(x_1^{\alpha}, x_1^{\beta}) \\ x_1^{\alpha} \text{ and } x_1^{\beta} \in [0; 1]}} \left[\frac{g_{2\text{phases}}^{\text{M}}(T, P, \mathbf{z}, \mathbf{x}^{\alpha}, \mathbf{x}^{\beta})}{RT} \right] \quad (11)$$

Relative stabilities of single and 2-phase systems are illustrated in Figure 2d,e. Figure 2d highlights that the single-phase binary system under consideration is in a liquid state for any $z_1 \leq 0.38$ and in a gaseous state for any $z_1 > 0.38$. This change of single-phase state along the composition axis induces a particular shape of the $\frac{g_{1\text{phase}}^{\text{M}}}{RT}$ versus z_1 curve, making it possible to draw a double tangent characterizing the presence of a vapor–liquid equilibrium (the equilibrium compositions are denoted x_1 and y_1). This double tangent, which is the locus of points $(z_1; g_{2\text{phases}}^{\text{M}}(T_0, P_2, \mathbf{z}, \mathbf{x}^{\alpha}, \mathbf{x}^{\beta}))$, is drawn in Figure 2e. As expected, for $x_1 \leq z_1 \leq y_1$, it is observed that the straight line $g_{2\text{phases}}^{\text{M}}(T_0, P_2, \mathbf{z}, \mathbf{x}^{\alpha}, \mathbf{x}^{\beta})$ versus z_1 (i.e., the double tangent) is located below the $g_{1\text{phase}}^{\text{M}}(T_0, P_2, \mathbf{z})$ versus z_1 curve. Consequently, for $z_1 \in [x_1; y_1]$, the two-phase state is stable whereas single-phase states are not stable.

To sum up, Figure 2d,e shows that the binary system at T_0 and P_2

- is in a single-liquid state for $z_1 < x_1$ (the single gas phase is not stable and it is not possible to find a two-phase state such that $g_{2\text{phases}}^{\text{M}} < g_{\text{liq}}^{\text{M}}$ in the composition range $[0; x_1]$);
- is in a two-phase state for $x_1 \leq z_1 \leq y_1$ (the single-liquid and single-gas phases are not stable in this composition range since it is possible to find x_1 and y_1 values such that $g_{2\text{phases}}^{\text{M}}(T_0, P_2, \mathbf{z}, x_1, y_1) < g_{1\text{phase}}^{\text{M}}(T_0, P_2, \mathbf{z})$ with $g_{1\text{phase}}^{\text{M}} = \min\{g_{\text{liq}}^{\text{M}}, g_{\text{gas}}^{\text{M}}\}$);

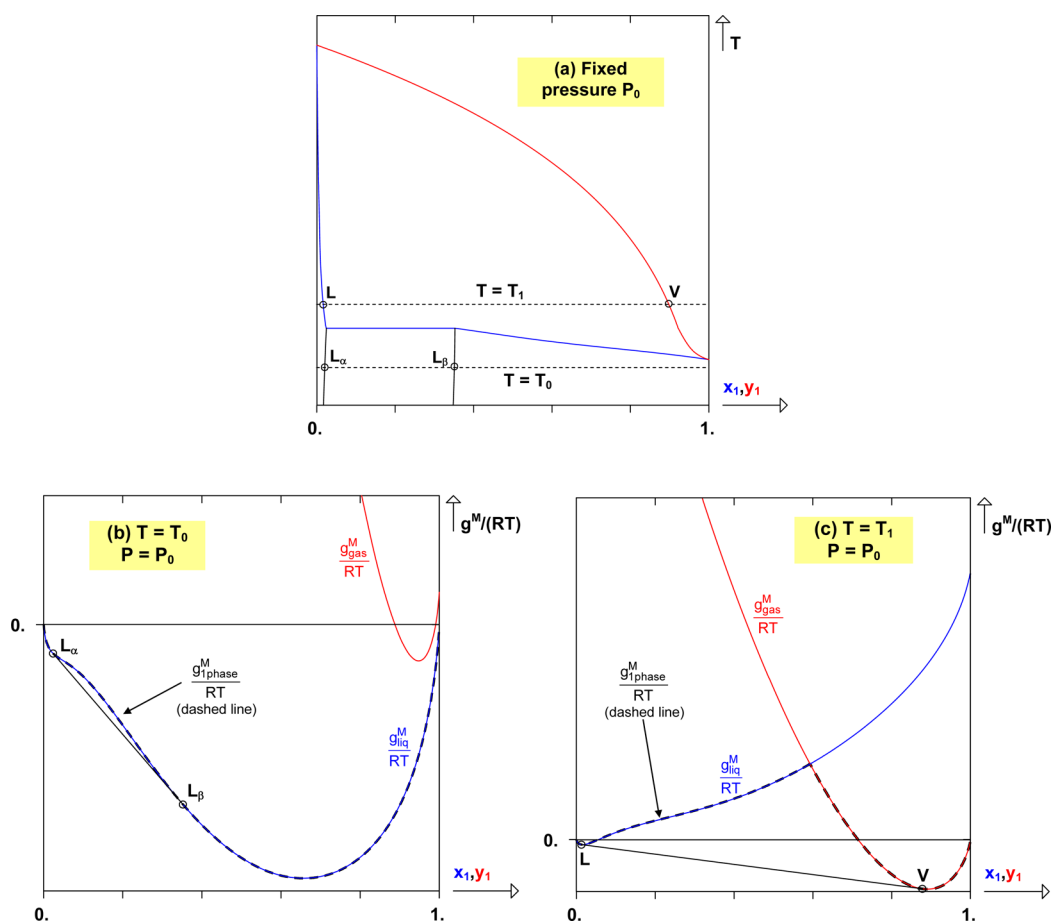


Figure 3. General shapes of isothermal–isobaric $g_{1\text{phase}}^M(T, P, \mathbf{z})/(RT)$ versus z_1 curves producing two-phase equilibria in binary systems.

- is in a single-gas state for $z_1 > y_1$ (the single-liquid phase is not stable and it is not possible to find a two-phase state such that $g_{2\text{phases}}^M < g_{\text{gas}}^M$ in the composition range $[y_1; 1]$).

Liquid–Liquid versus Vapor–Liquid Phase Equilibria.

According to the previous section, when, at specified T and P , a binary mixture exhibits one 2-phase state, it is always possible to draw a double tangent to the isothermal–isobaric $g_{1\text{phase}}^M(T, P, \mathbf{z})$ versus z_1 curve (this is a graphical consequence of the 2-phase equilibrium condition⁶). However, the shape of this curve gives important information on the nature of the phase equilibrium (liquid–liquid or liquid–vapor). To illustrate this fact, a binary system showing both vapor–liquid and liquid–liquid equilibria at a same pressure P_0 (see the isobaric phase diagram presented in Figure 3a) is considered. The shapes of the isothermal–isobaric $g_{1\text{phase}}^M(T, P, \mathbf{z})$ versus z_1 curves plotted at (T_0, P_0) and (T_0, P_1) are now discussed.

- Configuration 1 (liquid–liquid equilibrium, denoted LLE): at P_0 and $T = T_0$, the binary system exhibits a liquid–liquid equilibrium. In such a case, the $g_{1\text{phase}}^M(T_0, P_0, \mathbf{z})$ versus z_1 curve is rigorously identical to the $g_{\text{liq}}^M(T_0, P_0, \mathbf{x})$ versus x_1 curve as shown in Figure 3b (note that, for any composition value, the gas phase is not stable and $g_{\text{liq}}^M(T_0, P_0, \mathbf{x}) < g_{\text{gas}}^M(T_0, P_0, \mathbf{y})$). As expected, a double tangent can be drawn on the $g_{\text{liq}}^M(T_0, P_0, \mathbf{x})$ versus x_1 curve (see the straight line $L_\alpha L_\beta$ in Figure 3b); this liquid–liquid double tangent is made possible due to the presence of 2 inflection points on the same $g_{\text{liq}}^M(T_0, P_0, \mathbf{x})$ versus x_1 curve.

- Configuration 2 (VLE): as shown previously in Figure 2 and as highlighted in Figure 3c, the crossing of the curves $g_{\text{liq}}^M(T_1, P_0, \mathbf{x})$ versus x_1 and $g_{\text{gas}}^M(T_1, P_0, \mathbf{y})$ versus y_1 induces a vapor–liquid equilibrium (L and V are the end points of the corresponding double tangent).

This classification of $g_{1\text{phase}}^M(T, P, \mathbf{z})$ versus z_1 curves is essentially valid at low temperature and low pressure (far from critical phenomena). For instance, in the vicinity of binary mixture critical points, vapor–liquid equilibria can be induced by the presence of 2 inflection points on isothermal–isobaric $g_{1\text{phase}}^M(T, P, \mathbf{z})$ versus z_1 curves.

Focus on Particular Solutions of the Minimization Problem (Eq 11). As an important feature of eq 9, for $\mathbf{x}^\alpha = \mathbf{x}^\beta = \mathbf{z}$, the 2-phase Gibbs energy change on mixing and the 1-phase Gibbs energy change on mixing are rigorously equal:

$$\frac{g_{2\text{phases}}^M(T, P, \mathbf{z} = \mathbf{x}^\alpha = \mathbf{x}^\beta)}{RT} = \frac{g_{1\text{phase}}^M(T, P, \mathbf{z})}{RT} \quad (12)$$

Note that eq 12 could have been also derived from the lever rule. As a consequence, in the case where the stable state of a binary system at (T, P, \mathbf{z}) is a single phase (i.e., 2-phase states are not stable and are thus associated with Gibbs energy change on mixing values such that $g_{2\text{phases}}^M(T, P, \mathbf{z}, \mathbf{x}^\alpha, \mathbf{x}^\beta) \geq g_{1\text{phase}}^M(T, P, \mathbf{z})$), the resolution of the minimization problem (eq 11) returns the particular solution: $\mathbf{x}^\alpha = \mathbf{x}^\beta = \mathbf{z}$ (called trivial solution hereafter).

However, it must be noted that the reciprocal statement is not always true: if the solutions of the optimization problem are such that $\mathbf{x}^\alpha = \mathbf{x}^\beta = \mathbf{z}$, the binary system is not necessarily in a 1-phase

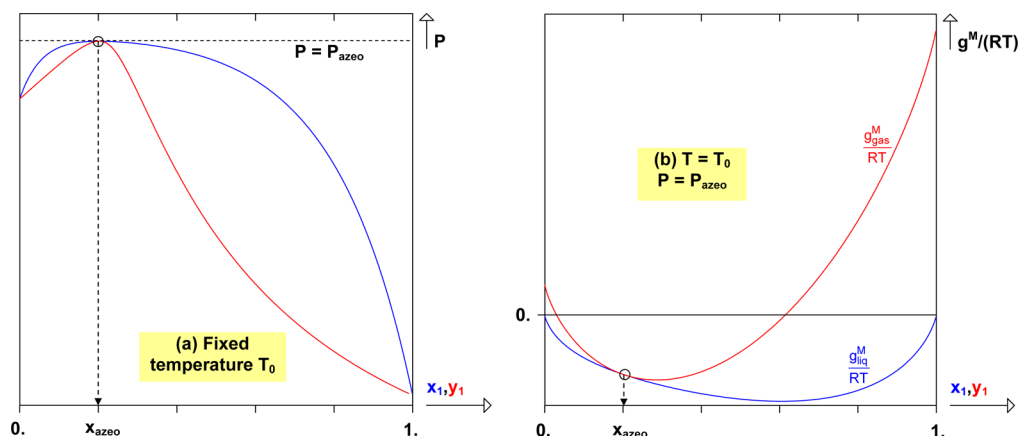


Figure 4. (a) Isothermal phase diagram of a binary system showing azeotropy (temperature T_0); (O) azeotropic point. (b) $g_k^M(T, P, \mathbf{z})$ versus z_1 and $g_{\text{gas}}^M(T, P, \mathbf{z})$ versus z_1 curves plotted at T_0 and P_{azeo} (azeotropic pressure).

state. For instance, let us address the case of a binary system showing azeotropy (see Figure 4a); the azeotropic pressure and composition are denoted P_{azeo} and x_{azeo} , respectively. Although numerically unlikely, the search for stable 2-phase equilibria at $(T_0, P_{\text{azeo}}, x_{\text{azeo}})$ will return the trivial solution since the two end points of the double tangent are superimposed at an azeotropic point (see Figure 4b). In such a case, the trivial solution is not associated with a single-phase system. Similar conclusions could be drawn for binary systems at fixed T, P, \mathbf{z} exhibiting liquid–vapor or liquid–liquid critical points.

APPLICATION TO THE CONSTRUCTION OF ISOBARIC FLUID-PHASE DIAGRAMS AT GIVEN PRESSURE

Isobaric phase diagrams are generated by performing successive PT flash calculations based on a Gibbs energy minimization procedure. The minimization problem to be solved is summarized by eqs 9 and 11 and requires models for estimating the Gibbs energy changes on mixing of the liquid and gas phases. In the present study, a γ – ϕ approach is used: liquid phases are represented by the NRTL activity-coefficient model whereas gas phases are assumed to behave as perfect gases (note that, according to a previous study,⁷ a distinction is made between perfect gas and ideal gas).

General Expressions of the Molar Gibbs Energy Change on Mixing of the Liquid and Gas Phases Using the γ – ϕ Approach

Activities are introduced to express the total molar Gibbs energy changes on mixing of a single phase:

$$\frac{g_k^M(T, P, \mathbf{z})}{RT} = z_1 \cdot \ln a_1^k(T, P, \mathbf{z}) + z_2 \cdot \ln a_2^k(T, P, \mathbf{z}) \quad (13)$$

$k \in \{\text{liq, gas}\}$

Note that activities are defined for both liquid and gas phases (which may appear unusual in this latter case). According to Privat and Jaubert,⁷ in order to apply the double-tangent construction and to perform stability analyses, the expression of the chemical potential of a given component in the liquid and gas phases (or equivalently, the activity expressions) must use the same reference state. They wrote: “When the two phases in equilibrium are not in the same aggregation state (e.g. a liquid phase in equilibrium with a gaseous phase) [...] it is compulsory that the pure-component reference state used to render the

chemical potential of a component i is the same in the two phases”. The expressions of the component activities in the liquid and gas phases were derived by selecting, as reference state, the corresponding pure-component actual stable state at the same temperature and pressure as the mixture;⁶ in eqs 14 and 15, γ_i and P_i^{sat} denote the activity coefficient of component i in the liquid phase (estimated using an activity-coefficient model) and the vapor pressure of pure i (estimated using an empirical correlation), respectively:

- If $P \geq P_i^{\text{sat}}(T)$:

$$\begin{cases} a_i^{\text{liq}}(T, P, \mathbf{z}) = z_i \cdot \gamma_i(T, \mathbf{z}) \\ a_i^{\text{gas}}(T, P, \mathbf{z}) = \frac{P \cdot z_i}{P_i^{\text{sat}}(T)} \end{cases} \quad (14)$$

- If $P < P_i^{\text{sat}}(T)$:

$$\begin{cases} a_i^{\text{liq}}(T, P, \mathbf{z}) = \frac{P_i^{\text{sat}}(T) \cdot z_i \cdot \gamma_i(T, \mathbf{z})}{P} \\ a_i^{\text{gas}}(T, P, \mathbf{z}) = z_i \end{cases} \quad (15)$$

Models for Activity Coefficients and Vapor Pressures

The classical 3-parameter NRTL model is considered for the estimation of the activity coefficients in liquid phase.⁸

$$\begin{cases} \ln \gamma_1(T, x_1) = x_2^2 \left[\tau_{21} \left(\frac{G_{21}}{x_1 + x_2 G_{21}} \right)^2 + \frac{\tau_{12} G_{12}}{(x_2 + x_1 G_{12})^2} \right] \\ \ln \gamma_2(T, x_1) = x_1^2 \left[\tau_{12} \left(\frac{G_{12}}{x_2 + x_1 G_{12}} \right)^2 + \frac{\tau_{21} G_{21}}{(x_1 + x_2 G_{21})^2} \right] \\ x_2 = 1 - x_1 \\ \tau_{12} = b_{12}/(RT) \text{ and } \tau_{21} = b_{21}/(RT) \\ G_{12} = \exp(-\alpha \tau_{12}) \text{ and } G_{21} = \exp(-\alpha \tau_{21}) \end{cases} \quad (16)$$

Numerical values of NRTL parameters for the 2 studied systems, *tert*-butanol (1) + water (2) and butan-2-one (1) + water (2), are reported in Table 1.

A classical Antoine equation is used to calculate pure-component vapor pressures:

$$\log_{10}(P_i^{\text{sat}}/\text{bar}) = A_i - \frac{B_i}{t/^\circ\text{C} + C_i} \quad (17)$$

Table 1. Parameters of the NRTL Model Used in This Study

binary systems	$b_{12}/(\text{J}\cdot\text{mol}^{-1})$	$b_{21}/(\text{J}\cdot\text{mol}^{-1})$	α
tert-butanol (1) + water (2)	3537.1	6440.50	0.5403
butan-2-one (1) + water (2)	4490.7	10337.2	0.4893

Pure-component Antoine parameters are provided in Table 2.

Table 2. Parameters of the Antoine Equation

molecules	A_i	B_i	C_i
tert-butanol	4.4809	1180.9	180.48
water	5.1962	1730.6	233.43
butan-2-one	4.1885	1261.3	221.97

Practical Implementation of the PT-Flash/Gibbs Energy Minimization Algorithm

The minimization problem to be solved is entirely defined by 2 sets of equations: the general formulation of a PT-flash calculation using a γ - ϕ approach is described by eqs 6, 9, 11, 13, 14, and 15; specific models are detailed in eqs 16 and 17; model parameters can be found in Tables 1 and 2.

The bioinspired krill herd algorithm is used to perform global optimization.⁹ Note that this technique was recently used by Moodley et al. for phase-stability analysis and phase-equilibrium calculations in reacting and nonreacting systems.¹⁰ In particular, they have shown that the krill herd algorithm outperforms most of other stochastic algorithms (genetic algorithm, covariant matrix adaptation evaluation strategy, shuffled complex evolution, firefly algorithm, modified cuckoo search) and matches the performances of the technique considered as the leading one (cuckoo search) for solving reacting and nonreacting phase-equilibrium problems.

This optimization algorithm is based on the simulated herding behavior of the krill crustacean: when krill are attacked by predators, individual krill are removed from the herd and krill density decreases. The motion of individual krill can be seen as a multiobjective process aimed at (a) reaching food and (b) increasing the krill density. This natural behavior has inspired an optimization algorithm to Gandomi and Alavi in which the objective function is interpreted as a distance between a krill individual and objectives (a) and (b). The variable vector is seen as the position vector of a krill individual. During the optimization process, the variable vector is varied following a Lagrangian model equation describing the motion of krill individuals. At the end of a process, krill individuals are supposed to be located near their optimal position. More details about this method can be found in the original paper.⁹

To apply the krill herd minimization method to the determination of a VLE at fixed T , P , and z (overall composition), parameters of the krill herd method were fixed as follows:

- The krill herd is assumed to be composed of 60 individual krill.
- The optimization variables x_1^α and x_1^β play a similar role and are actually interchangeable. In order to facilitate the convergence of the minimization process, the variable ranges of the 2 variables were dissociated by imposing the following constraints:

$$0 < x_1^\alpha < z_1 \quad \text{and} \quad z_1 < x_1^\beta < 1 \quad (18)$$

- Note that, if the final values of the variables are such that $x_1^\alpha \approx x_1^\beta \approx z_1$, it must be concluded that the mixture is in a 1-

phase state (at fixed T , P , and z , the azeotropic state and the critical state are numerically unlikely).

- A krill herd optimization process is made up of an initialization step and a motion process which is repeated until convergence is reached (i.e., until krill have reached their optimal positions). In our code, each VLE is calculated by running 150 krill herd optimization processes (each process is different since initial positions of the krill individuals are randomly affected). The final values of x_1^α and x_1^β are the optimal ones along the 150 optimization processes and along the 60 individual krill.

As mentioned in the Introduction, the present article relates a pedagogical experience taking the form of project-based learning: for the first time, master students were briefly initiated to the concepts of Gibbs energy minimization, PT-flash algorithm, and global optimization; they were invited to read a list of pedagogical documents, including the paper by Gandomi and Alavi,⁹ and then to participate in a question-and-answer session. Then, working in small groups and supervised by teachers, they were proposed to produce a general PT-flash algorithm based on Gibbs energy minimization similar to the one presented in Figure 5. In this algorithm, \mathbf{X} denotes the vector containing the 2 optimization variables (x_1^α and x_1^β). The optimal solutions over the 150 optimization processes are stored in \mathbf{X}_{best} .

This general algorithm, which includes optimization and thermodynamic blocks, was implemented using the Fortran 90 language (a code can be obtained by interested readers upon simple request sent to R. Privat's e-mail address). Regarding optimization aspects, the krill-herd routines were entirely deduced from the reading of the paper by Gandomi and Alavi.⁹

Example 1: Construction of the Phase Diagram of the tert-Butanol (1) + Water (2) System at 0.133 bar

The isobaric phase diagram of the tert-butanol (1) + water (2) system at 0.133 bar is represented in Figure 6 and shows as main singularity, an azeotropic point.

When the input values T , P , and z of the developed PT-flash algorithm (relying on a Gibbs energy minimization procedure) are such that the stable state of the binary system is a vapor-liquid equilibrium, the PT-flash algorithm returns the phase-equilibrium compositions (denoted x_1 and y_1). In other words, at given T , P , z such that the system is in a VLE state, a PT-flash tool provides the coordinates of a single bubble point ($x_1; T$) and a single dew point ($y_1; T$) at fixed P . The complete bubble and dew curves of an isobaric VLE diagram can thus be generated by repeating PT-flash calculation run at fixed P with well-chosen values of the two other input variables T and z . Due to the presence of an azeotropic point, the construction of the whole phase diagram was divided into two steps: (1) calculation of the part of the phase diagram located at $z_1 < z_1^{\text{az}}$ (where z_1^{az} denotes the azeotropic composition) and (2) calculation of the part of the phase diagram located at $z_1 > z_1^{\text{az}}$. For elaborating the first part of the phase diagram, students working on this project were invited to deduce the following algorithm (illustrated in Figure 7):

1. Initialization step:

- P is set at a fixed value.
- $\Delta T \leftarrow |T_{b,2}(P) - T_{b,1}(P)|/30$ (with $T_{b,i}(P)$, the boiling temperature of pure i at P)
- Search for the first VLE in the vicinity of pure-component 2 VLE: to do so, the temperature is fixed at $T = T_{b,2}(P) - \Delta T$ and the overall mole fraction z_1 is varied between 10^{-3} and 0.1 by step of 5×10^{-3}

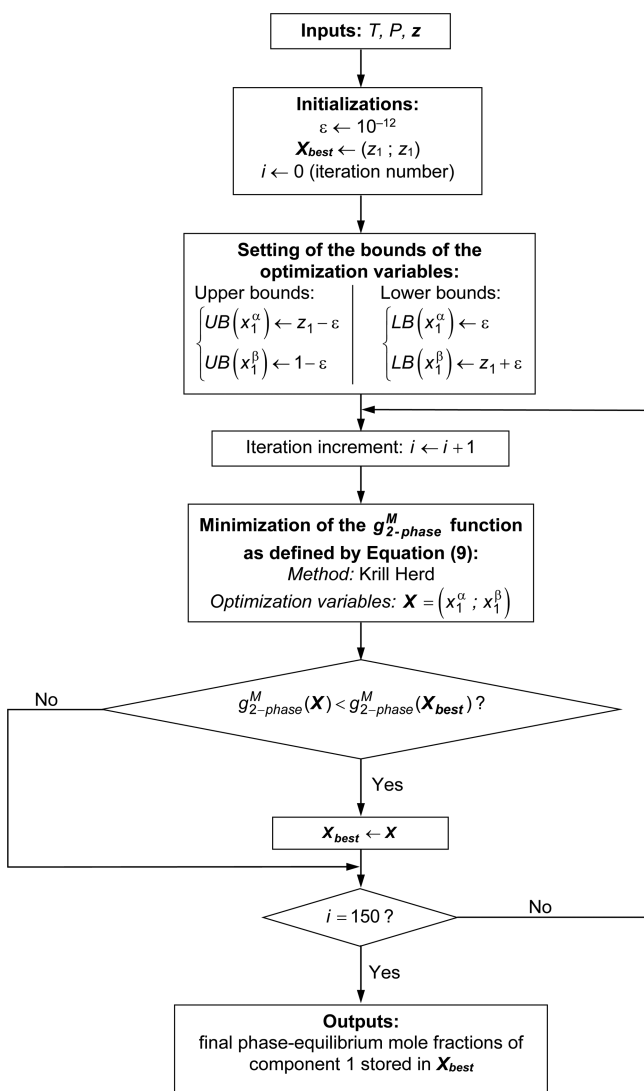


Figure 5. General algorithm for a PT-flash calculation based on Gibbs energy minimization.

until a VLE is found (liquid and gas compositions x_1 and y_1 are then returned by the flash algorithm).

- Run a PT-flash calculation having as input arguments

$$\begin{cases} z_1 \leftarrow \frac{1}{2}(x_1 + y_1) \\ T \leftarrow T - \Delta T \end{cases}$$

By determining new z_1 values following this way, the binary system remains in a 2-phase state, provided ΔT is low enough.

- If a VLE is found, save values of T , x_1 and y_1 and go back to step 2.

If a 1-phase state is observed,

- If $\Delta T > 10^{-5}$ K, go back to previous value of temperature ($T \leftarrow T + \Delta T$), change the ΔT value ($\Delta T \leftarrow \Delta T/10$), and go back to step 2.
- Else, the process is terminated. Plot T versus x_1 (bubble curve) and T versus y_1 (dew curve).

A similar algorithm can be used to construct the second part of the phase diagram (located at $z_1 > z_1^{az}$). The only difference with the previous algorithm lies in the initialization step since, in that

case, the first VLE is searched in the vicinity of pure-component 1 VLE.

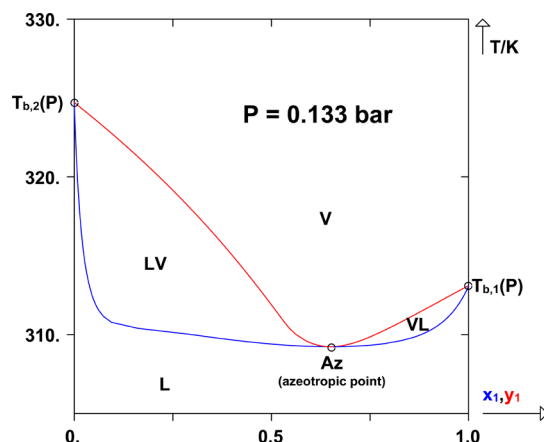


Figure 6. Calculated phase diagram of the *tert*-butanol (1) + water (2) system at 0.133 bar.

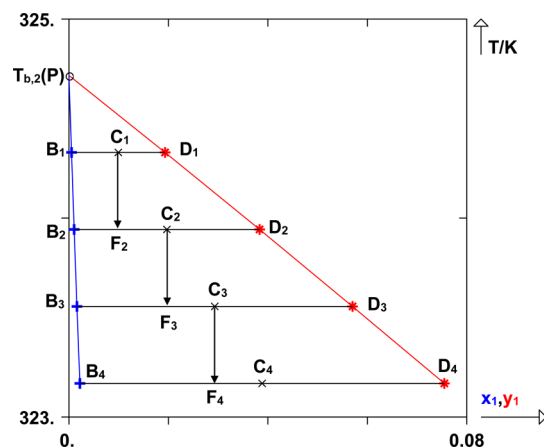


Figure 7. Illustration of the strategy used to build the phase diagram of the *tert*-butanol (1) + water (2) system at 0.133 bar by using the developed PT-flash algorithm. B and D: bubble and dew points. C: center of segment [BD]. Point F_i shows the input overall mole fraction used in the flash algorithm to calculate points B_i and D_i .

Example 2: Construction of the Phase Diagram of the Butan-2-one (1) + Water (2) System at 1.01325 bar

Top ranking students working on the aforementioned project were invited to compute a more complex phase diagram than the one exhibited by the *tert*-butanol (1) + water (2) system at 0.133 bar. They were invited to work on the phase-equilibrium behavior of the butan-2-one (1) + water (2) system at 1.01325 bar which exhibits, among other things, a homogeneous azeotropic point and a liquid–liquid region intersecting a vapor–liquid region through a liquid–liquid–vapor equilibrium line. This complex phase diagram is shown in Figure 8.

A similar algorithm to the one illustrated in Figure 7 can be used to calculate the regions surrounding the azeotropic point. The algorithm needs however to be slightly adapted to manage the presence of liquid–liquid and liquid–vapor regions surrounding a 3-phase line. This last one can be implicitly detected by an abrupt change of the compositions of the liquid or gas phases; to do so, the following criterion was used:

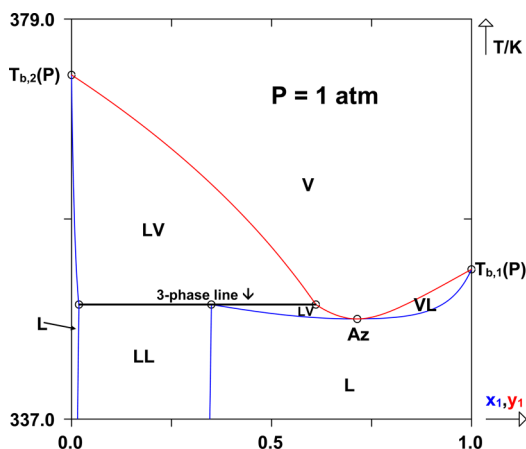


Figure 8. Calculated phase diagram of the butan-2-one (1) + water (2) system at 1.01325 bar.

$$\Delta xy > 0.4 \quad \text{with} \quad \Delta xy = \frac{|x_1 - x_1^{\text{old}}|}{x_1^{\text{old}}} + \frac{|y_1 - y_1^{\text{old}}|}{y_1^{\text{old}}}$$

Once an abrupt change of composition is identified, the temperature is set to its previous value ($T \leftarrow T + \Delta T$), the temperature step is decreased ($\Delta T \leftarrow \Delta T/10$), and the temperature is reaffected ($T \leftarrow T - \Delta T$); a new PT-flash calculation is then performed. The procedure is repeated until the 3-phase line temperature is determined with an accuracy better than 10^{-5} K. Once the 3-phase line is accurately calculated, the calculation of the remaining liquid–liquid and liquid–vapor regions is performed according to the algorithm presented above.

CONCLUSION

In this article, a methodology is proposed for teaching the fundamentals of Gibbs energy minimization. Although this technique could be applied to a variety of problems related to chemical-equilibrium or multiphase-equilibrium calculations, it was decided, for the sake of simplicity, to focus on the calculation of 2-phase equilibria in binary systems using the γ - ϕ approach. This class of thermodynamic problems can be reduced to a rather easy-to-solve minimization problem of a scalar function of 2 variables.

More concretely, the proposed methodology was successfully tested on a group of 100 master students through a transversal project aimed at developing computer skills, understanding the role of thermodynamic models (equations of state, activity-coefficient models) in the design of chemical engineering separation units, and implementing global optimization methods. It was seen that, through the indirect process of a computer program development, which necessarily involves the design, analysis, and implementation of specific problem solving algorithms, the students were forced to study and understand concepts that would be otherwise tedious to teach in the framework of typical theoretical class sessions.

AUTHOR INFORMATION

Corresponding Authors

*E-mail: romain.privat@univ-lorraine.fr.

*E-mail: jean-noel.jaubert@univ-lorraine.fr.

Notes

The authors declare no competing financial interest.

REFERENCES

- (1) Sandler, S. I. *Chemical, Biochemical, and Engineering Thermodynamics*, 4th ed.; Wiley: Hoboken, NJ, 2006.
- (2) Smith, J. M.; Van Ness, H. C.; Abbott, M. M. *Introduction to Chemical Engineering Thermodynamics*, 7th ed.; International Ed.; McGraw-Hill Chemical Engineering Series; McGraw-Hill: Boston, MA, 2005.
- (3) Privat, R.; Jaubert, J.-N.; Privat, Y. A Simple and Unified Algorithm to Solve Fluid Phase Equilibria Using Either the Gamma-Phi or the Phi-Phi Approach for Binary and Ternary Mixtures. *Comput. Chem. Eng.* **2013**, *50*, 139–151.
- (4) Wai, C. M.; Hutchison, S. G. Free Energy Minimization Calculation of Complex Chemical Equilibria: Reduction of Silicon Dioxide with Carbon at High Temperature. *J. Chem. Educ.* **1989**, *66* (7), 546.
- (5) Borge, J. Reviewing Some Crucial Concepts of Gibbs Energy in Chemical Equilibrium Using a Computer-Assisted, Guided-Problem-Solving Approach. *J. Chem. Educ.* **2015**, *92* (2), 296–304.
- (6) Jaubert, J.-N.; Privat, R. Application of the Double-Tangent Construction of Coexisting Phases to Any Type of Phase Equilibrium for Binary Systems Modeled with the Gamma-Phi Approach. *Chem. Eng. Educ.* **2014**, *48* (1), 42–56.
- (7) Privat, R.; Jaubert, J.-N. Discussion around the Paradigm of Ideal Mixtures with Emphasis on the Definition of the Property Changes on Mixing. *Chem. Eng. Sci.* **2012**, *82*, 319–333.
- (8) Renon, H.; Prausnitz, J. M. Estimation of Parameters for the NRTL Equation for Excess Gibbs Energies of Strongly Nonideal Liquid Mixtures. *Ind. Eng. Chem. Process Des. Dev.* **1969**, *8* (3), 413–419.
- (9) Gandomi, A. H.; Alavi, A. H. Krill Herd: A New Bio-Inspired Optimization Algorithm. *Commun. Nonlinear Sci. Numer. Simul.* **2012**, *17* (12), 4831–4845.
- (10) Moodley, K.; Rarey, J.; Ramjugernath, D. Application of the Bio-Inspired Krill Herd Optimization Technique to Phase Equilibrium Calculations. *Comput. Chem. Eng.* **2015**, *74*, 75–88.